SUPPLEMENTARY INFORMATION

Size-Controlled Synthesis of Bioinspired Polyserotonin Nanoparticles with Free Radical Scavenging Property

Keuna Jeon,[ab] Nesha May O. Andoy,[b] Christian W. Schmitt,[c] Yilei Xue, [b†]
Leonie Barner,[c] Ruby May A. Sullan[ab]*

[a] Department of Physical and Environmental Sciences, University of Toronto Scarborough, 1065 Military Trail, Toronto, ON, M1C 1A4, Canada. E-mail: ruby.sullan@utoronto.ca
[b] Department of Chemistry, University of Toronto, 80 St. George St., Toronto, ON, M5S 3H6, Canada
[c] School of Chemistry and Physics, Centre for Materials Science, Institute for Future Environments, Queensland University of Technology (QUT), 2 George Street, Brisbane, Queensland, 4000 Australia
[†] Department of Chemistry, The Hong Kong University of Science and Technology, Clear Water Bay, Kowloon, Hong Kong

1 Experimental Details

1.1 Synthesis of Polyserotonin Nanoparticles (PSeNP). Serotonin hydrochloride (Tokyo Chemical Industry America), sodium hydroxide (NaOH, ACP Chemicals), and trisaminomethane (Tris), potassium phosphate dibasic, potassium phosphate monobasic, ammonium hydroxide (NH_4OH) from Sigma Aldrich, were used without further purification. Polyserotonin nanoparticles (PSeNP) were synthesized via three routes: (1) Tris buffer, (2) aqueous NH_4OH, and (3) aqueous NaOH—at different pHs: pH 9, pH 10, and pH11 (Fig. S1A). In route (1), Tris (10 mM) buffer was first adjusted to pH 9, 10, and 11 with NaOH before the addition of serotonin hydrochloride (2 mg/mL). In routes (2) and (3), serotonin hydrochloride (2 mg/mL) was dispersed in MilliQ-H_2O and the pH was adjusted with either NH_4OH (2) or NaOH (3) to pH 9, 10, and 11. The vials were then set aside at room temperature (23 °C). To shorten the time required to synthesize PSeNP in Tris (10mM) buffer, the buffer was heated to 60 °C (heated synthesis) before serotonin hydrochloride (2mg/mL) was added. To investigate the influence of buffer composition on PSeNP synthesis, synthesis was also performed using phosphate buffered saline (PBS, 10mM) and bicine buffer (10mM) at pH 9 (60 °C). In monitoring the kinetics of nanoparticle formation, PSeNP were synthesized at 60 °C at pH 8.5, pH 9, and pH 10.

1.2 Purification. In all synthetic routes, nanoparticles are collected via centrifugation (Eppendorf 5804R) at 20817rcf for 10 mins at 4 °C. For synthesis done at RT, once the colour of the reaction mixture changed to slightly brown (inset in Fig. S1A) with corresponding absorbance of ~0.7 at 475 nm, nanoparticles were collected, i.e., the bottom layer (Fig. S1A bottom), and further washed

with Milli-Q water 3×. The supernatant from this first centrifugation, i.e., the top layer (Fig. S1A top), was set aside at room temperature for 1 more day.

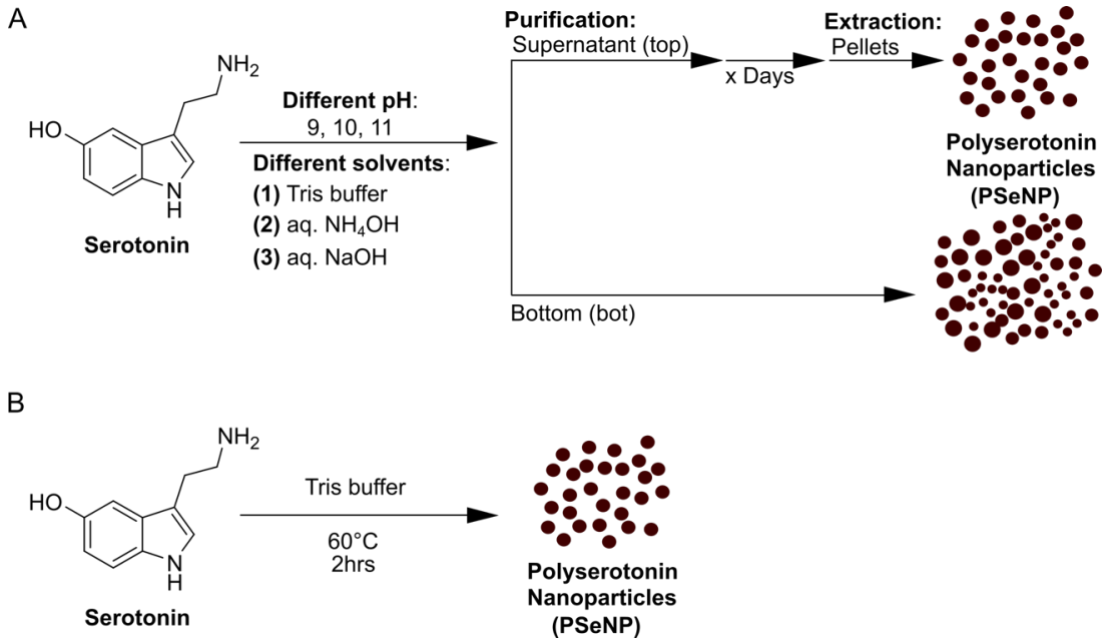

Fig. S1 Schematic of polyserotonin nanoparticle (PSeNP) synthesis in (A) various conditions at room temperature (23 °C) and optimized synthesis in (B) Tris buffer at 60 °C (heated synthesis).

1.3 Spectroscopic Characterization. Optical absorption spectroscopy of aqueous PSeNP solutions was performed to characterize the absorption spectrum of the nanoparticles. Absorption spectra from UV to Near-IR (NIR) regions were recorded using an Agilent Technologies Cary 60 apparatus while Fourier-transform infrared (FTIR) spectra using Bruker Alpha FTIR Spectrometer with Platinum ATR. To determine if PSeNP has free radical centers, electron paramagnetic resonance (EPR) spectra were recorded using a Bruker X-band CW EMX EPR spectrometer equipped with a 10" electromagnet and an ER 4123D resonator. To characterize the elemental composition of the nanoparticle surface, X-ray photoelectron spectroscopy (XPS) analysis was performed under incident conditions, the X-ray penetration depth being lower than 5 nm (ultrathin layer method). XPS samples were prepared by first casting PSeNP powder on silicon wafers to cover a 1×2 mm^2 area. A Thermo Fisher Scientific system (K-Alpha and Theta Probe) was used to obtain XPS results for polyserotonin and analysed using Avantage software. Survey (wide) scans were carried out over 1200 – 0 eV binding energy range with 1.0 eV steps at a pass energy of 200 eV. High-resolution spectra of C 1s, O 1s, and N 1s regions were recorded using a pass energy of 25 eV. Three scans were performed for survey spectra and 20 scans for each of the high-resolution spectra. Three scans were performed for survey spectra and 10 scans for each of the high-resolution spectra.

1.4 Dynamic Light Scattering (DLS) and Zeta Potential Analysis. The size of the growing nanoparticles was monitored using dynamic light scattering (DLS, NanoBrook Omni, Brookhaven Instruments) while the surface zeta potential was determined using phase analysis light scattering (PALS, NanoBrook Omni, Brookhaven Instruments). Measurements were conducted in buffer solutions at room temperature at an angle of 90° for dilute polyserotonin suspensions.

1.5 Electron Microscopy Imaging. To visualize the nanoparticles, scanning electron microscopy (SEM, Hitachi S530 with Quartz PCI version 8 image management system for Fig. 1C, Fig. S2, and Fig. S5), and transmission electron microscopy (TEM, Hitachi H7500 with iTEM version 5.2 software for Fig. 1C inset, Fig. 3A, Fig. S4, and Fig. S6) were performed. Synthesized polyserotonin were drop-casted onto Au-coated Si wafers for SEM imaging. Images were analysed with ImageJ 1.52a to estimate the diameter of the nanoparticles.

1.6 Assay for Antioxidant Activities. DPPH radical scavenging activity of PSeNP were measured according to established methods on DPPH radical scavenging assay.[1] DPPH (2,2-diphenyl-1-picrylhydrazyl) (0.1mM) solution was freshly prepared in 95% ethanol before use. A small aliquot of concentrated PSeNP in water (6.25–300 µL) was mixed with 4mL of DPPH solution. The amount of PSeNP investigated for antioxidant activities were back calculated using the standard curve at wavelength 800nm (Fig. S14). The free radical scavenging activity was evaluated by monitoring the absorbance at 516 nm as soon as it was mixed and subsequently for every 30 min for a total of 3 hrs. DPPH radical scavenging activity was calculated as $\mathrm{I} = [1 - (A_i - A_j)/A_c] \times 100\%$, where A_c is the absorbance of DPPH solution without PSeNP, A_i is the absorbance of the samples of PSeNP mixed with DPPH solution, and Aj is the absorbance of the PSeNP without DPPH solution. All the samples were kept in the dark in between UV-Vis readings.

2 Discussion Details

2.1 Purification of Polyserotonin Nanoparticles (PSeNP)

The purification step has been performed as shown in Fig. S1 schematic to isolate a monodisperse distribution of PSeNP, as measured by DLS and visualized by SEM and TEM (Fig. S2, Fig. 1C and Fig. S4). The bottom layer was extracted once the colour of the solution changed from a clear and colourless to brown, which corresponds to an absorbance reading of ~0.7 or greater at 475 nm, as shown for day 1 in Fig. S3A and inset. The supernatant was set aside for another day, which then resulted in a monodispersed PSeNP (Fig. S2 Top, Fig. 1C and Fig. S4).

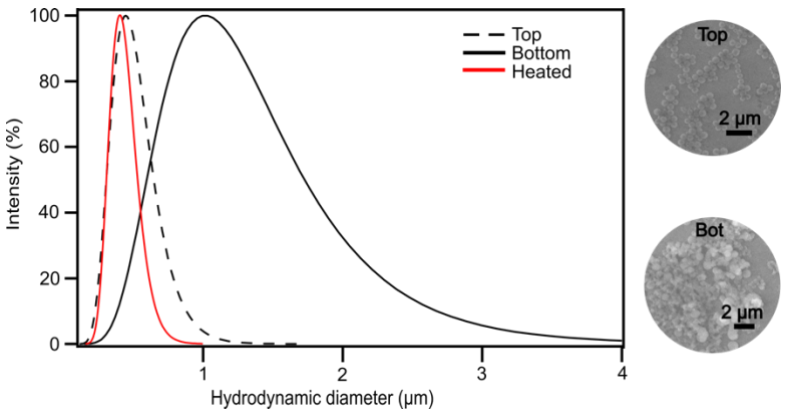

Fig. S2 DLS measurement of PSeNP synthesized in Tris buffer at pH 9 at room temperature (23 °C) with corresponding SEM images of Top and bottom layer (bot). Scale bar is 2 μm.

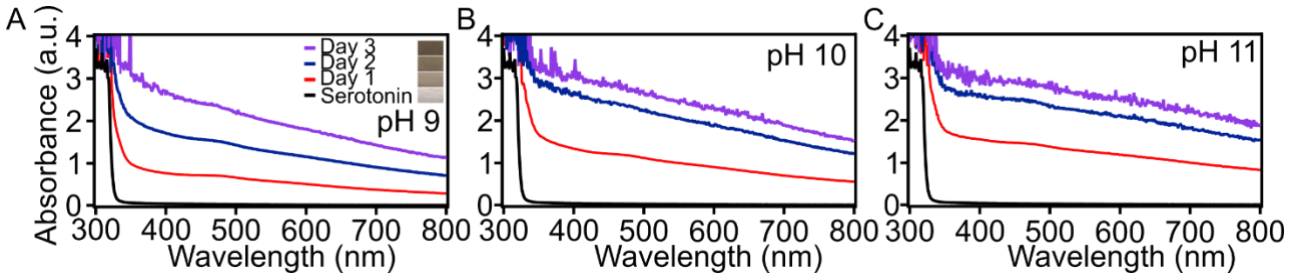

Fig. S3 UV-Vis spectroscopy of PSeNP synthesized in Tris buffer at (A) pH 9, (B) pH 10, and (C) pH 11 from left to right. The black curve corresponds to serotonin monomer while the red, blue, and purple curves correspond to PSeNP (Top layer, Fig. S1 and S2) extracted at day 1, day 2, and day 3, respectively. Inset in A shows the corresponding solution colour for each day for PSeNP synthesis at pH 9.

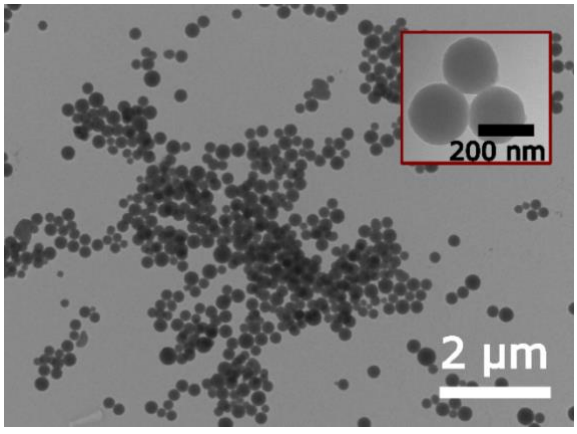

Fig. S4 TEM image of PSeNP synthesized in Tris at pH 9 with a zoomed in view in inset (red box).

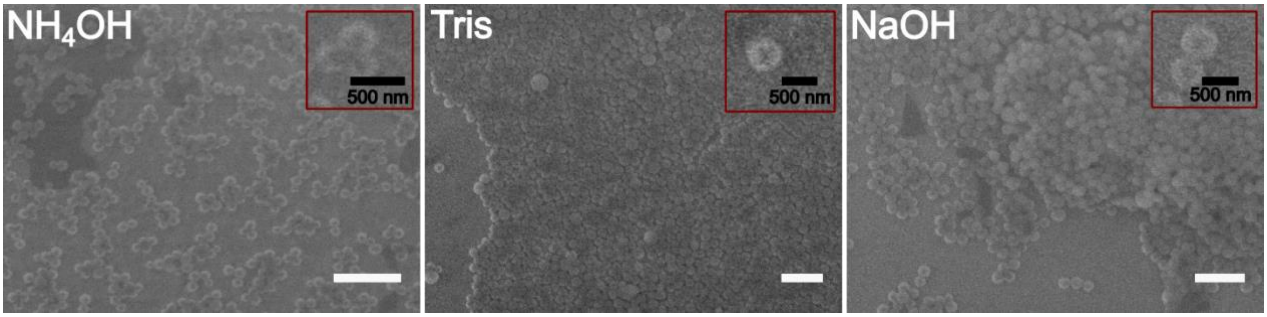

Fig. S5 SEM images of PSeNP synthesized at pH 10 in NH_4OH (2 days), Tris (6 days), and NaOH (3 days). The days correspond to the time at which PSeNP (top layer) were harvested. Scale bar is 2μm.

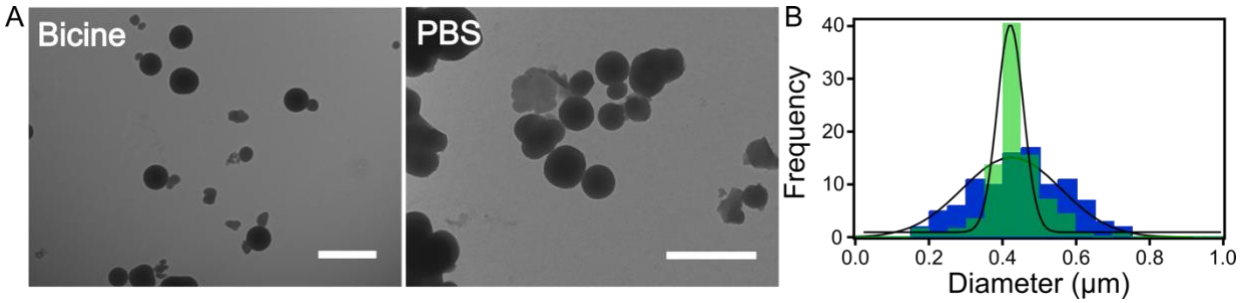

Fig. S6 (A) TEM images of PSeNP synthesized at pH 9, 60 °C in 10mM (A) bicine buffer and (B) phosphate buffer (PBS) following the same reaction conditions as Tris buffer shown in Fig. S1B; scale bar is 1μm. (C) Corresponding histograms of spherical-shaped PSe formed in bicine (green, 421± 37nm) and in PBS (blue, 425 ± 134nm).

2.2 FTIR Analysis

In the FTIR spectrum, oxidation of the monomer is apparent at 3000–3500 cm^{-1}, for all polymers synthesized in different solvent systems (Fig. 2B). The peak at 1519 cm^{-1}, which is due to the stretching of N-H bond, while present in the monomer serotonin, is not visible in all polyserotonin across different solvent systems.[2]

2.3 Kinetics of Polyserotonin Nanoparticle Formation

We monitored the kinetics of polyserotonin nanoparticle formation synthesized at room temperature (RT, 23 °C) and at an elevated temperature (60 °C) at pH 8.5, 9 and 10 via DLS measurements (Fig. S7) and UV-Vis spectroscopy (Fig. S9). Our results show that as the pH increases, the rate of serotonin oxidation also increases, as seen from the faster rate of increase in broad absorbance the higher the pH (Fig. S9 B-D). Our DLS measurements also show that higher pH leads to faster formation of nanoparticles. At pH 10, it only takes ~15 min for the count rate to increase from <200 kcps to >400kcps, indicating the formation

of highly scattering materials, i.e., nanoparticles (Fig. S7C-D, red squares), from polymers of serotonin that does not scatter well. This is in contrast to pH 8.5, where the process takes ~120 min, an 8-fold difference from pH 10 (Fig. S7C-D, blue triangles). Furthermore, we also observed that at the time when a dramatic shift in scattering intensity is apparent, the size of the nanoparticles that were measured for all three pHs were already >100 nm and are comparable in size (Fig. S7A, S7C). This suggests that more than the size, the pH has a greater effect on the kinetics of "seed" formation. However, the final pH-dependence of the nanoparticle size that we observed (i.e., bigger at higher pH) comes from the pH-dependence of the rate of particle growth. Fig. S7A shows that the rate at which the particle grows from its initial seed size increases with increasing pH—at pH 10 the seed grew to more than 2× its initial size after 4hrs, while nanoparticles at pH 9 only increased by a few tens of nanometers, and those at pH 8.5 barely grew at all. This led to bigger nanoparticle size at higher pH. This faster rate of growth at higher pH is most likely driven by the presence of more oxidized serotonin oligomers (or monomers), as evidenced by faster increase in absorbance at 475 nm the higher the pH of the solution (Fig. S9). The presence of more serotonin oxidation products means more material can bind to the surface of the "seed nanoparticles" leading to faster growth, giving rise to bigger nanoparticles.

The heated synthesis at pH 8.5 and pH 10, in addition to the heated synthesis at pH 9, was performed to check whether the nanoparticle size is heavily influenced by the buffering capacity of the buffer used (Tris). These two pH values allow us to compare the pH dependence of the nanoparticle size within and outside the ideal buffering capacity range (pH 7.1-9.1) of Tris: pH 8.5 vs. pH 9 (within) and pH 9 vs. pH 10 (outside). PSENP synthesized at pH 8.5 are smaller (~95 ± 26 nm, Fig. S10A) than those synthesized at pH 9 (~ 201 ± 49 nm, Fig. S10B), which in turn are smaller than those synthesized at pH 10 (size ~387 nm, Fig. S7A, red squares). Note that in this size comparison, the nanoparticles were extracted after 4 hrs of synthesis as the particles at pH 8.5 at 2hrs, seem to have not yet fully formed. We note that while the size of PSENP formed at pH 8.5 is smaller than at pH 9 (Fig. S10), pH 9 results in a faster synthesis (2 hrs) and higher yield (4% for pH 9 vs. 1.3% for pH 8.5).

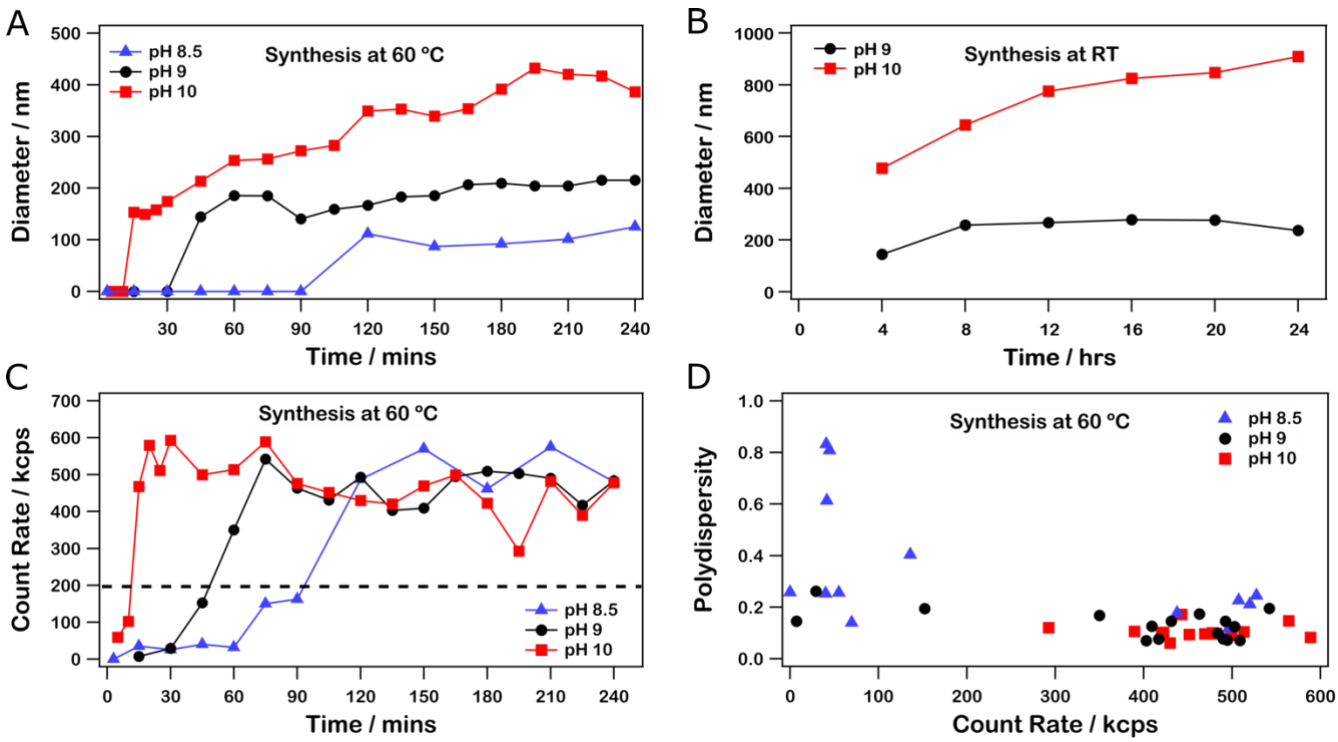

Fig. S7 Kinetics of polyserotonin nanoparticle formation at (A) 60 °C (heated synthesis) and (B) room temperature (23 °C)—at pH 8.5, pH 9, and pH 10. Diameters represent the mean MSD values obtained from DLS runs. Note the different time axis in A and B. (C) Evolution of count rate with time and (D) scatter plot between count rate and polydispersity of PSeNP synthesized at 60 °C.

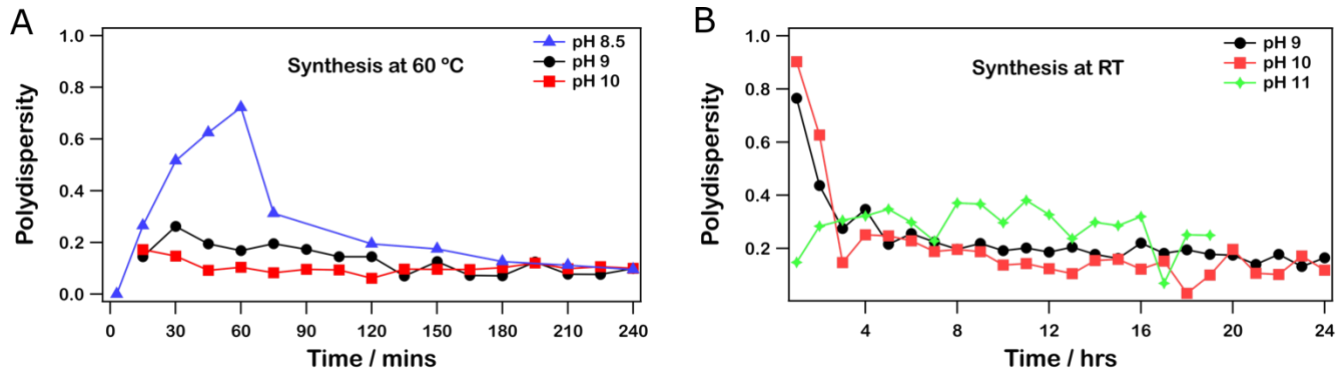

Fig. S8 Evolution of polydispersity (PDI) with time of polyserotonin nanoparticles synthesized at (A) an elevated temperature of 60 °C and (B) at room temperature (23 °C) obtained from DLS measurement. Note the different time axis in A and B.

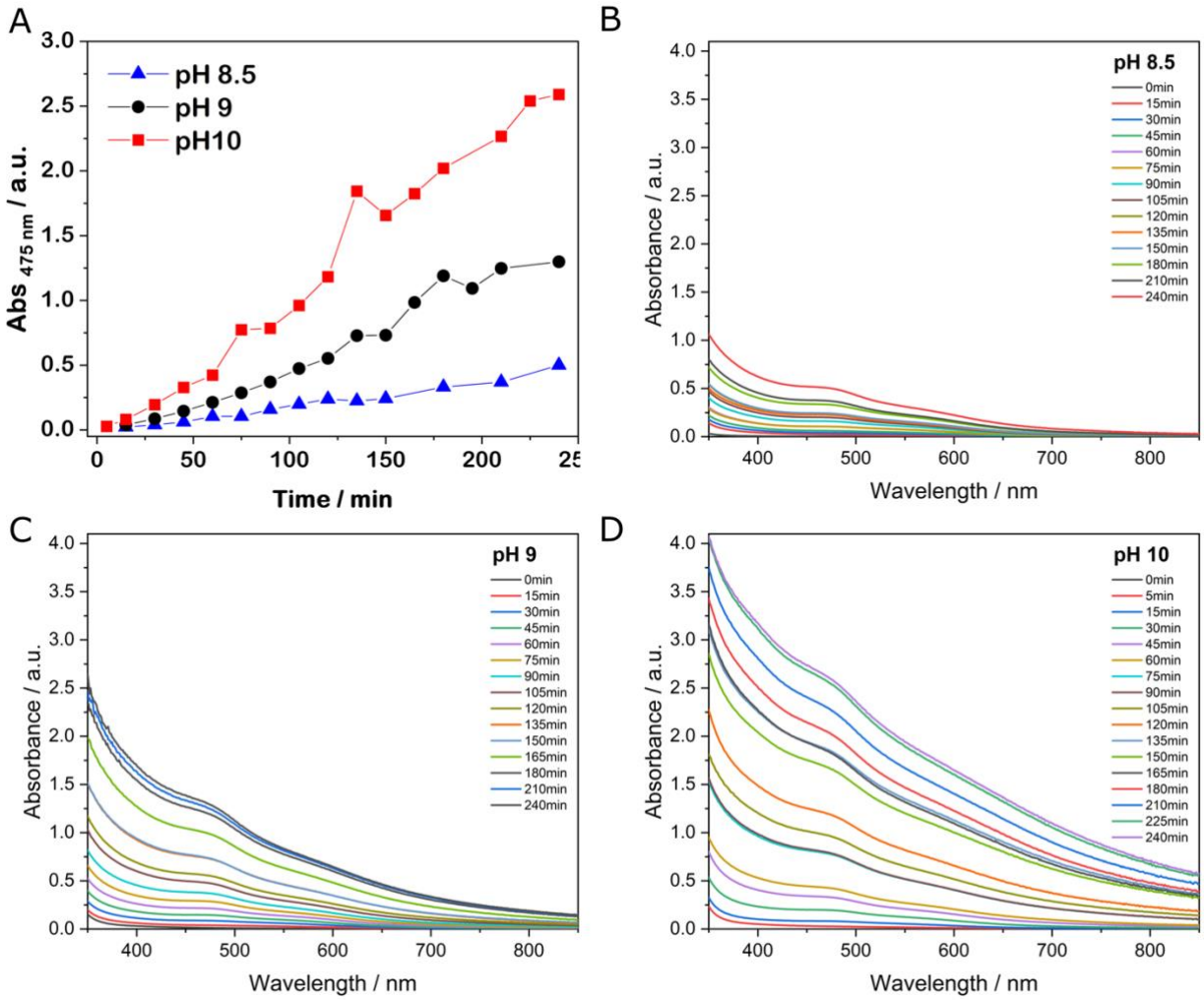

Fig. S9 (A) Absorbance of PSeNP synthesis solution at 475 nm, monitored over time. Values are obtained from UV-Vis spectra of heated synthesis at (B) pH 8.5, (c) pH 9, and (D) pH 10).

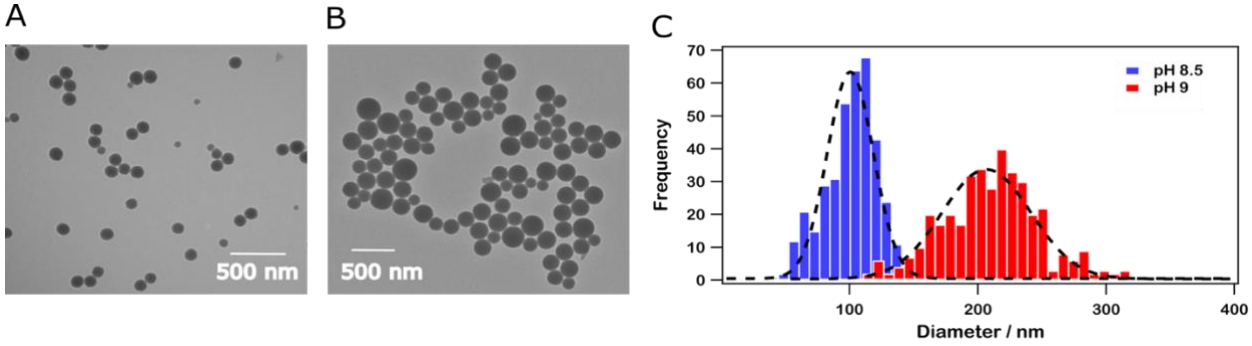

Fig. S10 PSeNP size increases with increasing pH. TEM images of PSeNP synthesized at 60 °C using Tris buffer (A) pH 8.5 and (B) pH 9, harvested after 4 hrs. (B) Corresponding histogram of size distribution with mean diameters of ~95 ± 26 and ~207 ± 49 nm, for pH 8.5 and pH 9, respectively, from Gaussian fits.

2.4 XPS Analysis

Comparison between polyserotonin and serotonin: X-ray photoelectron spectroscopy (XPS) was performed to identify the chemical composition and bonding on the surface of PSeNP. From the survey spectra we can conclude that the serotonin monomers have indeed been oxidized during the polymerization process (ESI Fig. S11).

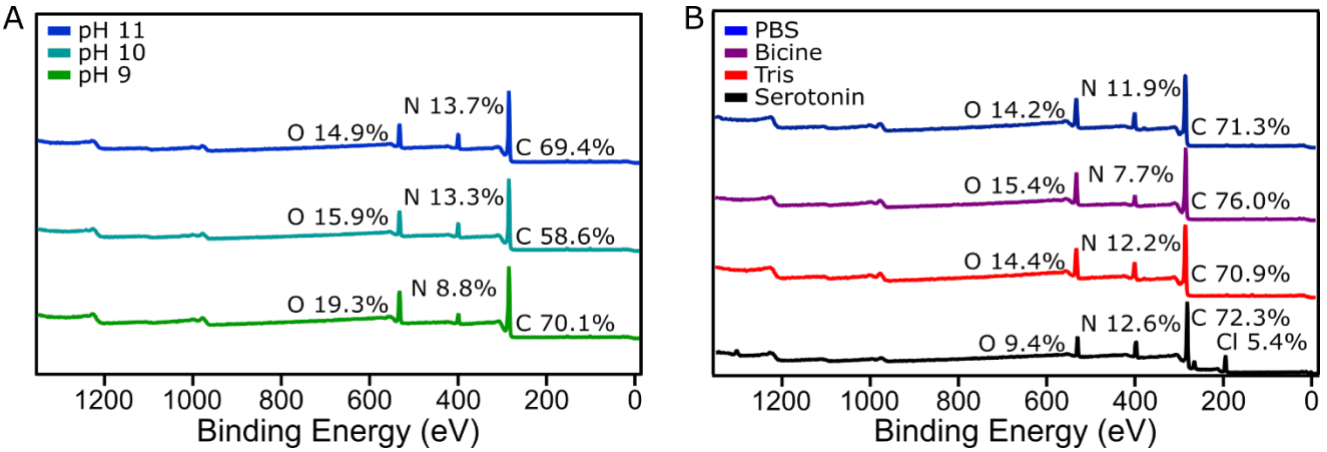

Fig. S11 Wide scan XPS comparison of polyserotonin synthesized (A) from the bottom in Tris pH 9 (green), pH 10 (turquoise), pH 11 (blue) without heat and (B) from the top in PBS (blue), bicine (purple), and Tris (red) in pH 9 with heat and serotonin monomers (black).

High-resolution scan of C 1s regions for serotonin monomers gave three peaks corresponding to C-H/C-NH_2 (284 eV, *purple*), C-O/C-N (286 eV, *green*), and C=O/C=N (287 eV, *blue*); whereas polyserotonin had all of these three peaks, with addition of $\pi \rightarrow \pi^*$ (289 eV, *military green*), and an increase in C=O/C=N (286 eV, *blue*) species (Fig. 3D).[3] The high-resolution scan of N 1s regions for polyserotonin showed a significant increase in abundance of secondary amine (401 eV, *purple*) with significant decrease of imines (399 eV, *purple*), and primary amines (402 eV, *blue*); where the presence of the last two species can be found higher than secondary amines in serotonin monomer.[3] Interestingly, O 1s regions showed the presence of three species in both serotonin and polyserotonin where there was an increase in O=C (531 eV, *purple*), a decrease in both H-O-C (534 eV, *blue*), and O-C (532 eV, *green*).[4] The increases of O=C, C=O/C=N, and $\pi \rightarrow \pi^*$ peaks from O 1s and C 1s with decreases of =N-R and primary amines from N 1s spectra in the polyserotonin is a good indication that the serotonin is using up the primary amine group to polymerize and oxidize, respectively. Complementary to this, the decrease in H-O-C and significant increase in O=C suggest that oxidation utilizing the hydroxyl group occurs but not all the hydroxyl group is being used to polymerize allowing some hydroxyl groups to be available on the surface PSeNP allowing further surface modifications[3] if desired.

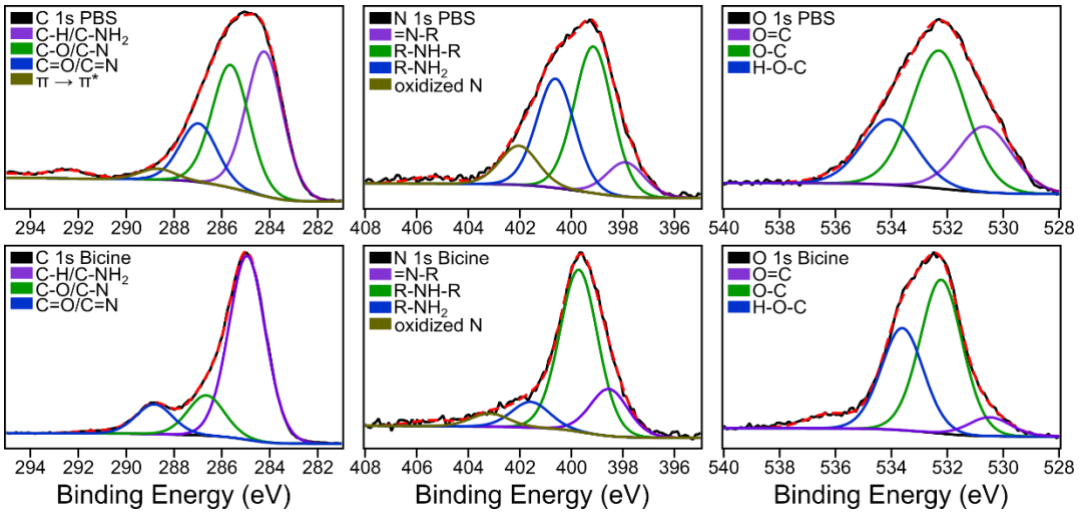

Fig. S12 High resolution XPS scan of the C 1s, O 1s, and N 1s peaks from left to right for polyserotonin nanoparticles synthesized in PBS (upper panel) and in Bicine buffer (lower panel) at 60 °C. Polyserotonin synthesized under different base components undergo similar oxidation process but with slight differences in surface functionalities afforded by the different base systems.

Comparison between polyserotonin nanoparticles formed in different buffer solvents: When comparing the polyserotonin formed in different solvent buffer systems, significant difference in O 1s high resolution scan of all three and difference in C 1s and N 1s spectra of phosphate buffer compared to the other two solvents (ESI Fig. S12). This may be due to the presence of amine groups in the solvent system that interacts with the monomer as bicine and Tris buffer systems have tertiary and primary amine groups, respectively. In N 1s high resolution spectra from phosphate buffer the primary amine (*blue*) peak remained while the imine peak drastically decreased compared to the serotonin monomer (Fig. 3D); whereas the bicine and Tris allowed the primary amines to be utilized in the formation of polyserotonin. In addition, the profile of the three O 1s peaks in phosphate buffer stayed similar to the monomer while the bicine buffer allowed more hydroxyl groups to be left when the tris buffer allowed more O=C bonds to form. This suggests that the solvents also interact with the monomers and induce different mechanisms when forming polyserotonin.

Comparison between heated and non-heated polyserotonin: The polyserotonin formed with the presence of heat (Fig. 3D lower panel) has increased amount of C-O/C-N (*green*) peak in the C 1s high resolution spectra compared to the non-heated polyserotonin (ESI Fig. S13 bottom panel). In O 1s high resolution spectra, the profile of the peaks in both from the heated and non-heated polyserotonin is very similar. However, a significant difference in the abundance of the secondary amine (*green*) peak is present in N 1s spectra of the polyserotonin from the non-heated synthesis. This suggests that without the presence of heat the amines get incorporated in the polymerization; whereas the formation of C-O occurs faster forming polyserotonin with the presence of heat.

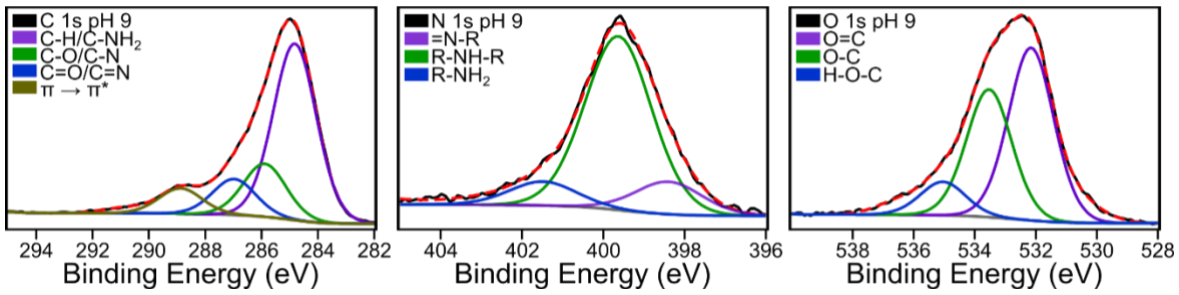

Fig. S13 High resolution XPS scan of the C 1s, O 1s, and N 1s peaks of polyserotonin nanoparticles synthesized in Tris buffer pH 9 at room temperature (23 °C).

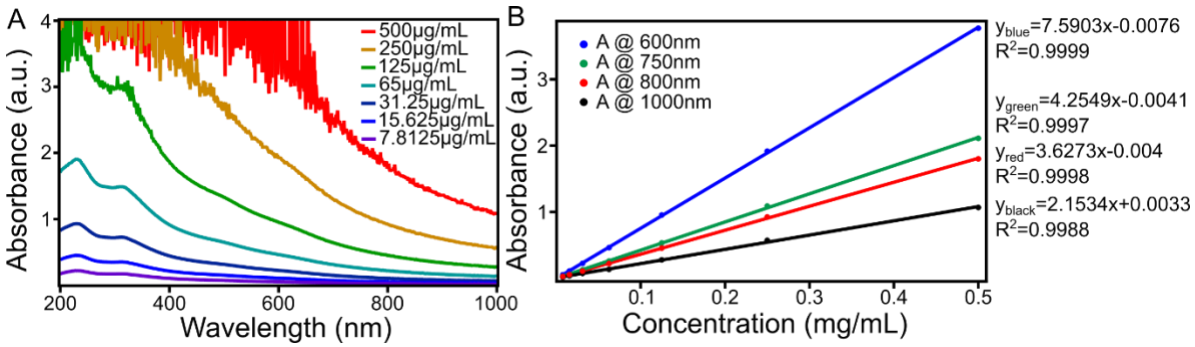

Fig. S14 (A) UV-vis absorbance spectra of PSeNP with different concentrations. B. A linear relationship for the optimal absorbance at 600nm (blue), 750nm (green), 800nm (red), and 1000nm (black) as a function of the concentration of PSeNP with corresponding equation of the line of best fit with R^2.

3 Electronic Supplementary Information References

1 K. Y. Ju, Y. Lee, S. Lee, S. B. Park and J. K. Lee, *Biomacromolecules*, 2011, **12**, 625–632.

2 W. Kiratitanavit, F. F. Bruno, Z. Xia, S. Yu, J. Kumar and R. Nagarajan, *J. Renew. Mater.*, 2019, **7**, 205–214.

3 N. Nakatsuka, M. M. Hasani-Sadrabadi, K. M. Cheung, T. D. Young, G. Bahlakeh, A. Moshaverinia, P. S. Weiss and A. M. Andrews, *ACS Nano*, 2018, **12**, 4761–4774.

4 G. P. López, D. G. Castner and B. D. Ratner, *Surf. Interface Anal.*, 1991, **17**, 267–272.